

# The influence of chain length and electrolyte on the adsorption kinetics of cationic surfactants at the silica–aqueous solution interface

R. Atkin,<sup>a,1</sup> V.S.J. Craig,<sup>b</sup> E.J. Wanless,<sup>a,\*</sup> and S. Biggs<sup>a,2</sup>

<sup>a</sup> *Discipline of Chemistry, School of Environmental and Life Sciences, The University of Newcastle, Callaghan, NSW 2308, Australia*

<sup>b</sup> *Department of Applied Mathematics, Research School of Physical Sciences and Engineering, Australian National University, Canberra, ACT 0200, Australia*

Received 18 August 2002; accepted 12 June 2003

## Abstract

The equilibrium and kinetic aspects of the adsorption of alkyltrimethylammonium surfactants at the silica–aqueous solution interface have been investigated using optical reflectometry. The effect of added electrolyte, the length of the hydrocarbon chain, and of the counter- and co-ions has been elucidated. Increasing the length of the surfactant hydrocarbon chain results in the adsorption isotherm being displaced to lower concentrations. The adsorption kinetics indicate that above the cmc micelles are adsorbing directly to the surface and that as the chain length increases the hydrophobicity of the surfactant has a greater influence on the adsorption kinetics. While the addition of 10 mM KBr increases the CTAB maximal surface excess, there is no corresponding increase for the addition of 10 mM KCl to the CTAC system. This is attributed to the decreased binding efficiency of the chloride ion relative to the bromide ion. Variations in the co-ion species (Li, Na, K) have little effect on the adsorption rate and surface excess of CTAC up to a bulk electrolyte concentration of 10 mM. However, the rate of adsorption is increased in the presence of electrolyte. Slow secondary adsorption is seen over a range of concentrations for CTAC in the absence of electrolyte and importantly in the presence of LiCl; the origin of this slow adsorption is attributed to a structural barrier to adsorption.

© 2003 Elsevier Inc. All rights reserved.

*Keywords:* Optical reflectometry; Surfactant; Adsorption; Kinetics; Silica

## 1. Introduction

The physicochemical characteristics of a surfactant monomer in solution determine the hydrophobicity of the molecule and the morphology of the surfactant aggregate. Changes in the structure of surfactant aggregates can be related to variations in the packing parameter, induced by altering the effective physical dimensions of the monomer (e.g., chain or headgroup size) or the solution conditions (electrolyte or temperature) [1].

The hydrocarbon chain length is of critical importance in determining the adsorption behavior of a surfactant. Goloub and Koopal [2] demonstrated that for adsorption to amorphous silica, increasing the chain length of the monomer by

four methylene units, from C<sub>12</sub> to C<sub>16</sub>, lowers the concentration at which characteristic features of the isotherm occur by approximately an order of magnitude. This corresponds to the reduction in solution cmc. Lajtar et al. [3] noted a qualitatively similar effect upon the addition of only two methylene units. The addition of electrolyte has an influence similar to increasing the hydrocarbon chain length. Electrolyte “salts out” the hydrocarbon chains of the surfactant and therefore results in adsorption at lower concentrations. Additionally, ion binding and charge screening influence the kinetics of adsorption and the packing of surfactant monomers into aggregates.

The influence of counterion identity, as well as surfactant and electrolyte concentration, on the adsorbed layer morphology of CTA<sup>+</sup> was investigated in the previous study of Velegol et al. [4] using AFM and optical reflectometry. For CTAB, it was shown that when the surfactant concentration was increased from 0.9 × cmc to 10 × cmc the adsorbed layer morphology changed from short rods to cylindrical micelles. This effect was consistent regardless of whether 10 mM KBr was present or absent, although added electrolyte did reduce

\* Corresponding author.

*E-mail address:* [erica.wanless@newcastle.edu.au](mailto:erica.wanless@newcastle.edu.au) (E.J. Wanless).

<sup>1</sup> Current address: School of Chemistry, University of Bristol, Cantock's Close, Bristol, BS8 1TS, UK.

<sup>2</sup> Current address: School of Process, Environmental and Materials Engineering, University of Leeds, Leeds, LS2 9JT, UK.

the spacing between the surface aggregates. When the counterion was changed from bromide to chloride, the CTAC surface aggregates were approximately spherical for both concentrations, and once again the presence of electrolyte did not significantly change the aggregate structure. These results were rationalized by the greater binding efficiency of bromide over chloride [5–7]. This leads to a reduction in the headgroup area and enables bromide ions to stabilize the lower curvature cylindrical surface aggregates. Using optical reflectometry, it was shown that the change in surface aggregate structure from spheres to cylinders (for CTAC and CTAB, respectively) corresponded to the surface excess increasing by two thirds.

Subramanian and Ducker [8] also investigated the effect of various electrolytes on the adsorbed structure of CTA<sup>+</sup> and have extended this explanation. In this case the authors interpreted similar results on the basis of the “hardness” of the ion. It was found that soft, polarizable (e.g., Br<sup>−</sup>) ions were more effective than hard counterions (e.g., CH<sub>3</sub>COO<sup>−</sup>, Cl<sup>−</sup>) at inducing shape changes in admicelles, namely a sphere-to-cylinder transition. It was suggested that as hard anions strongly bind water they are relatively unavailable for binding to surfactant cations. Soft counterions, which interact weakly with water, associate more readily with the surfactant. Binding of counterions lowers the repulsive force between headgroups, permitting the formation of the lower curvature cylindrical aggregates.

In the current investigation the influence of the surfactant chain length, the species of counterion and the presence of electrolyte on the adsorption kinetics and equilibrium surface excess of quaternary ammonium surfactants on hydroxylated silica is studied. The influence of co-ions will also be studied, as it has been suggested [8] that hard co-ions (e.g., Li<sup>+</sup>) should have the lowest affinity for the silica and micelle surfaces and therefore have the least effect on adsorption phenomena. Importantly, identical substrates were used for all experiments, as comparison of results obtained in some previous adsorption investigations on silica have been complicated by variability in the properties of the substrate. This variability can arise from the method of substrate preparation [9–11] or the cleaning procedures prior to use [4,11,12]. Additionally, Goloub et al. have suggested that these problems have often been extenuated by poor control of the solution conditions, especially for depletion experiments [13].

Particular attention will be given to the adsorption kinetics, which has not previously been studied as a function of chain length for ionic surfactants or co-ion type. Optical reflectometry is well suited to kinetic studies of adsorption as it has high temporal resolution and the experimentally determined adsorption rates can be compared to the diffusion limited flux to the surface. This allows the adsorption mechanism to be commented upon [14]. The adsorption kinetics of cationic C<sub>16</sub> surfactants has been extensively described previously [4,9,10]. In general, adsorption times were found to be rapid, on the order of a few seconds, save for a narrow concentration range in the vicinity of the critical sur-

face aggregation concentration (csac), where long-term secondary increases in adsorption were noted. This region of the isotherm is known as the slow adsorption region (SAR). The SAR is a mechanistic cusp between two thermodynamically stable interfacial structures [9,10]. The effect of counterion and co-ion variation on the SAR will also be investigated in this paper.

## 2. Materials and methods

Cetyltrimethylammonium bromide (C<sub>16</sub>TAB or CTAB), myristyltrimethylammonium bromide (C<sub>14</sub>TAB or MTAB), dodecyltrimethylammonium bromide (C<sub>12</sub>TAB or DTAB), and cetyltrimethylammonium chloride (CTAC) (all with purity greater than 99%) were obtained from Aldrich, recrystallized twice from acetone, and freeze-dried prior to use. KBr, KCl, and LiCl (Analytical Grade) were obtained from Aldrich and were oven-baked for 24 h at 600 °C to remove organic contaminants. All water used was filtered, distilled, and passed through a Millipore filtration unit before use. The cmc values for each surfactant were determined from conductivity measurements.

Silicon wafers were baked at 1000 °C for 100 min in an oxygen atmosphere to produce an oxide layer (SiO<sub>2</sub>). Surfaces with lower hydroxyl group density are obtained upon baking due to condensation reactions at the silica surface that result in the formation of siloxane bonds [15]. When used in this state we call the silica pyrogenic. Pyrogenic silica will slowly rehydroxylate when immersed in water resulting in what is termed hydroxylated silica. Hydroxylated silica was prepared here by soaking pyrogenic silica in water for 48 h, followed by treatment with 10 wt% NaOH for 30 s, rinsing in water and then ethanol before drying under a nitrogen stream. All silica used in this study was of the hydroxylated form. The thickness of the oxide layer present on the silicon wafer was determined ellipsometrically using an Auto EL-II automatic ellipsometer (Rudolf Research) to be 165 ± 1 nm. The refractive indices of silica and silicon used in the determination of surface excess were 1.46 and 3.8, respectively.

The optical reflectometry technique used follows that used by Dijt et al. [16] and has been detailed in a previous paper [9]. Reflectometry relies on the changes in the reflective properties of a substrate upon adsorption of a material. In a typical reflectometry experiment the cell initially contains only water (or electrolyte solution) while a stable baseline is recorded. Surfactant (or surfactant and electrolyte) solution is then passed into the cell via a two-way valve and the change in the ratio of the two perpendicular polarizations of the laser beam recorded, which is proportional to the surface excess. The reflectometer is entirely contained in an incubator, allowing the temperature to be accurately maintained at 25 ± 0.1 °C.

The hydrodynamics and deposition of colloidal particles in a stagnation point flow have been investigated by Dabros and van de Ven [17]. The current investigation is concerned

only with their final equations describing diffusive mass transport, and simplifications that can be made when surfactant molecules are used in place of colloidal particles. The hydrodynamics associated with stagnation point flow are well defined. While the injected solution flows about the stagnation point, any exchange is diffusion limited. Thus, the rate of adsorption of surfactant to the silica surface is diffusion limited and defined by the equation

$$J = 0.766v^{1/3}R^{-1}D^{2/3}(\alpha Re)^{1/3}c, \quad (1)$$

where  $v$  is the kinematic viscosity,  $D$  is the diffusion coefficient,  $Re$  is the Reynolds number,  $c$  is the concentration of adsorbate, and  $\alpha$  is determined by the ratio  $h/R$ , where  $h$  is the distance between the surface and the inlet tube, and  $R$  is the radius of the tube. The values of the variables used in the calculation of the theoretical diffusion-limited flux were  $u = 0.0022$ ,  $R = 0.0013$ ,  $v = 8.93 \times 10^{-7}$ ,  $Re = 3.37$ ,  $a = 2 \times 10^{-9}$ ,  $h = 0.0015$ ,  $\alpha = 6$ , and the concentration of the surfactant solution in  $\text{kg m}^{-3}$ . The diffusion coefficients used for DTAB, MTAB, and CTAB monomers were  $6.02 \times 10^{-10}$ ,  $5.73 \times 10^{-10}$ , and  $5.50 \times 10^{-10} \text{ m}^2 \text{ s}^{-1}$ , as reported in [18]. The diffusion coefficient for CTAC was assumed to be the same as CTAB. The diffusion coefficient used for the micelles was  $8.36 \times 10^{-11} \text{ m}^2 \text{ s}^{-1}$ , which was calculated using a micelle radius of 2.9 nm [19]. At the concentrations of surfactant and electrolyte used in this study the diffusion coefficient of the micelles effectively remains unchanged [20]. While the diffusion coefficients do not vary greatly from one surfactant to the next, the difference in the surfactant cmc values has a significant influence on the calculated diffusion-limited flux. This is because at the cmc the rate of increase of the theoretical flux with concentration is decreased due to the slow diffusion of micelles when compared to monomers.

### 3. Results and discussion

#### 3.1. Surfactant chain length

Typical data for the adsorption of the three alkyltrimethylammonium bromide surfactants in 10 mM KBr are presented in Fig. 1. The general form of the adsorption data for DTAB and MTAB is essentially the same as that described earlier for CTAB [9]. In order to emphasize the fast kinetics of the adsorption process only a limited time period is presented. Before the introduction of surfactant, a baseline was first recorded using the solvent; in this case, a 10 mM KBr solution. Surfactant was then passed into the cell at 12.5 s resulting in a rapid increase in the surface excess, reaching equilibrium levels within approximately 6 s for all three surfactants. The equilibrium surface excess remained constant whilst surfactant solution was flowing into the cell. Upon 10 mM KBr being introduced into the cell, the surface excess rapidly dropped to levels below the detection capability

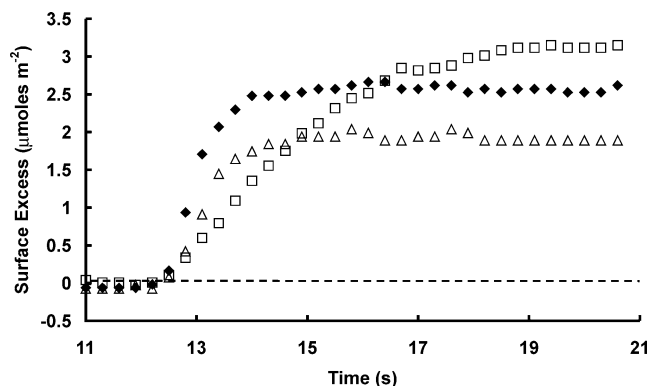


Fig. 1. Sample data for the adsorption of quaternary ammonium bromide surfactants at the silica–solution interface versus time in the presence of 10 mM KBr: 0.1 mM CTAB ( $\square$ ), 0.8 mM MTAB ( $\blacklozenge$ ), and 5 mM DTAB ( $\triangle$ ). These surfactant concentrations are approximately  $0.8 \times \text{cmc}$  of each surfactant in 10 mM KBr. The surfactant solution is first passed into the cell at  $\sim 12.5$  s, leading to adsorption. The plateau level of adsorption is maintained while the surfactant solution is flowing into the cell.

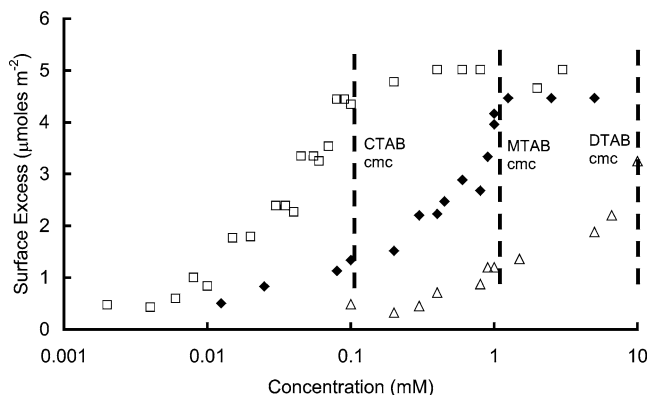


Fig. 2. Adsorption isotherms for CTAB ( $\square$ ), MTAB ( $\blacklozenge$ ), and DTAB ( $\triangle$ ) in the presence of 10 mM KBr. The dashed vertical lines represent the solution cmc for each surfactant.

ities of the instrument (not shown). Numerous experiments have been used to determine the adsorption isotherm.

In Fig. 2 the adsorption isotherms for DTAB, MTAB, and CTAB in 10 mM KBr are presented. There is an increase in the maximal surface excess with chain length and the adsorption isotherms are displaced to lower concentrations as the chain length is increased. This effect has been reported previously [2,3] and is attributed to the increased hydrophobicity imparted by the progressively longer hydrocarbon tail-groups. This promotes surface aggregate formation at lower surfactant concentrations and is directly analogous to the corresponding reduction in cmc observed in solution. The surface excess decreases in the order CTAB > MTAB > DTAB for all concentrations above  $0.1 \times \text{cmc}$ . Below this concentration the isotherms are coincident as a fraction of the cmc.

The isotherms are most conveniently divided into three regions: a charge neutralization region, a steeply increasing region, and a maximal surface excess region (not determined for DTAB). The presence of a fourth region [21], at low

surfactant concentrations, corresponding to surface excess values up to that required for neutralization of the native surface charge is not disputed. However, as these surface excess values are for the most part below the sensitivity of optical reflectometry, this region will not be examined here.

The magnitude of the surface excess in the charge neutralization region is approximately equal for the three surfactants and is most likely due to neutralization of the *native* surface charge [2]. This region of the isotherm will not be addressed here, as other techniques are more suitable for evaluating low surface excess values and the kinetic data for such low adsorption levels is unreliable.

Hydrophobic interactions, the magnitude of which are largely determined by the chain length, are important in determining the characteristics of the steeply increasing region of the adsorption isotherm as the length of the hydrocarbon tail is increased. The concentration at which the surface excess begins to increase appreciably is substantially reduced and the concentration range over which the increasing region occurs is decreased from 12 mM for DTAB [11], to 1 mM for MTAB, to 0.1 mM for CTAB, respectively. For the three chain lengths investigated in the presence of electrolyte, the increasing region of the isotherm is smooth and exhibits no discontinuities. This is not the case in the absence of electrolyte. For  $C_{16}$  surfactants, the surface excess increases abruptly between 0.5 and 0.6 mM, rising from 1.5 to  $3.5 \mu\text{mol m}^{-2}$  [9]. This is attributed to a transition from hemimicelle to admicelle surfactant structures. The smooth form of the isotherms obtained here for the three surfactants in electrolyte suggests that the background electrolyte stabilizes interfacial structures intermediate to the hemimicelle and the admicelle structures. However, the precise morphology of these aggregates is not clear. Attempts to image surfactant structures at low concentrations using atomic force microscopy have been largely unsuccessful. This is most likely due to the insufficiently repulsive interaction of the tip with the structures formed.

The critical surface aggregation concentration (csac) is the lowest concentration at which the maximal surface excess is obtained. It is found to be slightly higher than the solution cmc for CTAB and MTAB in the presence of 10 mM KBr. While the increase in surface excess above the cmc is small, this result is in contrast to results obtained in the absence of electrolyte [9,10,22]. When electrolyte is not present, the csac is approximately  $0.3\text{--}0.6 \times \text{cmc}$ . Whether the slight increase in surface excess above the cmc observed here is due to an increase in aggregate size or greater aggregate packing density is uncertain.

The kinetics of adsorption for DTAB, MTAB, and CTAB in 10 mM KBr are presented in Fig. 3. The initial adsorption rate is equal to the gradient of the linearly increasing region of an adsorption experiment (as per Fig. 1). For surface excess values up to approximately  $0.25 \mu\text{mol m}^{-2}$ , electrostatic interactions control the adsorption rate. At these surface excess values the error in the measured adsorption rate will be high, so these results are not reported here. For surfactant ad-

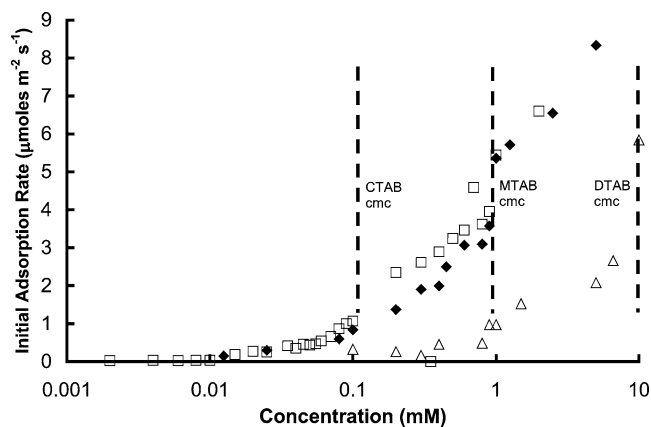


Fig. 3. Initial adsorption rate for CTAB (□), MTAB (◆), and DTAB (△) in the presence of 10 mM KBr. The dashed vertical lines represent the solution cmc for each surfactant in 10 mM KBr.

sorption that results in surface excess values of greater than  $0.25 \mu\text{mol m}^{-2}$ , electrostatic and hydrophobic interactions will contribute to the adsorption rate [14]. The higher the final surface excess, the greater the hydrophobic contribution will be. The analysis of adsorption rates in this work is conducted at concentrations where hydrophobic interactions are dominant. The errors in the surface excess associated with these measured kinetics are much less, of the order of  $0.1 \mu\text{mol m}^{-2}$ . As the contribution from electrostatic interactions will not vary greatly between surfactant concentrations, differences in the measured adsorption rates are, therefore, primarily a consequence of the level of hydrophobic interactions.

Generally, adsorption increases with concentration as is expected due to the increased flux of surfactant to the surface. However the *rate* of increase in adsorption rate with increasing concentration reveals details of the adsorption process. In the vicinity of the cmc there is an abrupt increase in the rate of adsorption for all of the surfactants. This has been observed previously [9,10] for  $C_{16}$  surfactants. This is due to the direct adsorption of micelles, which facilitates rapid and effective surface aggregate formation [14].

The comparison of the adsorption kinetics between the three surfactants is not as simple as it may first appear. For the comparison to be valid it is necessary that (a) comparisons be made, not at the same concentration but rather in the same region of the adsorption isotherm, and (b) the rate at which the surfactant is being delivered to the surface is appropriately accounted for. The first of these conditions is largely accomplished by normalizing the concentration axis by the cmc. The second is achieved by comparing the actual rate of adsorption to the theoretical diffusion limited flux to the surface. We express this ratio as the sticking ratio [9]. Put simply, a ratio of one means that every surfactant molecule that reaches the surface is adsorbed. An increasing sticking ratio with increasing concentration is indicative of cooperative adsorption and a decreasing sticking ratio with increasing concentration is indicative of competitive adsorption. On a charged hydrophilic surface, adsorption

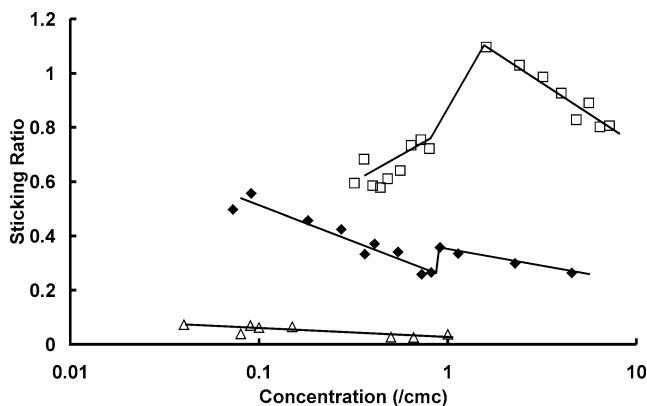


Fig. 4. Sticking ratio versus concentration normalized by the cmc for CTAB ( $\square$ ), MTAB ( $\blacklozenge$ ), and DTAB ( $\triangle$ ) in the presence of 10 mM KBr. The lines are drawn to guide the eye.

kinetics that are predominantly driven by electrostatic interactions will show competitive behavior, as surfactant molecules are required to compete for charged sites. Conversely, on a charged hydrophilic surface, adsorption kinetics that are driven predominantly by hydrophobic interactions will exhibit cooperative behavior. Therefore a plot of sticking ratio versus concentration normalized by the cmc enables kinetic data for surfactants of different chain lengths to be compared. The data of Fig. 3 is presented in this form in Fig. 4. Additionally, it must be remembered that the cmc values and therefore the actual concentration of monomer in solution is very different in the three cases.

With reference to Fig. 4, the first observation that can be made is that the magnitude of the sticking ratio increases with surfactant chain length. As the chain length increases the adsorption success increases substantially. Clearly, hydrophobicity is important in the initial stages of surfactant adsorption. This supports descriptions of adsorption that describe the various mechanisms of adsorption as operating concurrently [14].

Below the cmc, the sticking ratio for CTAB is seen to be increasing with concentration, indicating that the adsorption is cooperative and the kinetics predominantly hydrophobically driven, whereas the sticking ratio for MTAB and DTAB is decreasing with increasing concentration indicating that the adsorption process is competitive and predominantly electrostatically driven. This is further evidence that the hydrophobic interactions become increasingly important as the chain length increases.

For CTAB there is a clear and marked transition in the sticking ratio at the cmc. Above the cmc the sticking ratio is greater by approximately 35% than immediately below the cmc. This indicates that the presence of micelles in solution greatly increases the success of adsorption on a per monomer basis. We attribute this to the direct adsorption of micelles to the surface [9,10]. We also note that as the bulk surfactant concentration is increased and thereby the number of micelles in solution is increased the sticking ratio gradually falls. This is indicative of competitive adsorption

between micelles. Micelles will only adsorb in a single layer. Each adsorbing micelle will necessarily occupy a region of the surface and thereby reduce the area available for further adsorption and thereby inhibit adsorption of subsequent micelles.

A similar, though less marked, increase in sticking ratio at the cmc is observed for MTAB, of  $\sim 25\%$ . This is attributed to the greater concentration of monomers in solution. At the cmc there will be competition between monomers and micelles for adsorption. This will be more significant as the chain length decreases and the cmc and the relative number of monomers present increases. Hence the magnitude of the change in sticking ratio at the cmc decreases with decreasing chain length. Only one datum point is available at the cmc for DTAB. It was not possible to obtain more data above the cmc in this system due to optical artefacts associated with mixing induced by the large concentration of surfactant in solution.

### 3.2. Chloride versus bromide counterions

The adsorption isotherms on hydroxylated silica for CTAB and CTAC with no added electrolyte, CTAB in 10 mM KBr and CTAC in 10 mM KCl are presented in Fig. 5. For simplicity when describing the data, CTAB in 10 mM KBr and CTAC in 10 mM KCl will henceforth be referred to as “CTAB + KBr” and “CTAC + KCl.”

It is apparent in Fig. 5 that the maximal surface excess is less for CTAC than for CTAB: 2.5 versus  $3.5 \mu\text{mol m}^{-2}$ . This result agrees with data obtained by Velegol et al. [4], also using optical reflectometry, and is a consequence of the decreased binding efficiency of the chloride ion to the adsorbed aggregates relative to the bromide ion.

The addition of electrolyte to the CTAB system results in a shift of the isotherm to lower surfactant concentrations and an increase in maximal surface excess. This is attributed to electrostatic screening of headgroup charges and an increased level of counter-ion binding. Both effects lead to a closer packing of surfactant monomers into surface aggregates.

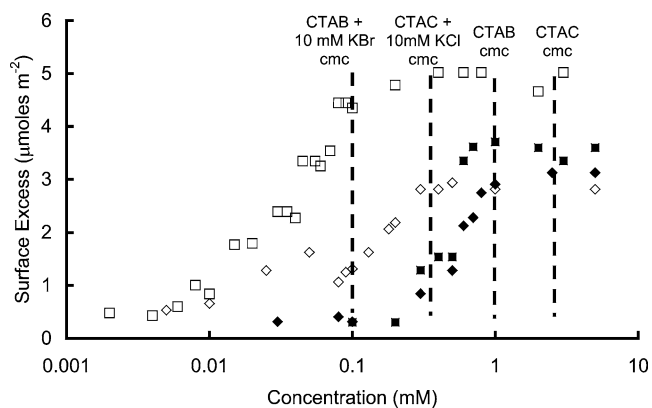


Fig. 5. Adsorption isotherms for CTAB in the presence ( $\square$ ) and absence ( $\blacksquare$ ) of 10 mM KBr and for CTAC in the presence ( $\diamond$ ) and absence ( $\blacklozenge$ ) of 10 mM KCl.

gates and an increase in surface excess. In comparison to the bromide ion, the chloride ion binds poorly, yet it has the same charge-screening properties; thus it is possible to separate the influence of the electrostatic screening from the ion binding in surfactant adsorption by comparing the effects of chloride and bromide counterions on surfactant adsorption. In contrast to the bromide system we find that the maximal surface excess is almost equivalent for CTAC and CTAC + KCl; however, the shift of the isotherm features to lower concentrations is still observed. The shift of the features is attributed to the electrostatic screening and the near equivalence in the maximal surface excess is attributed to the low ion-binding in the chloride system. Thus, the structure of adsorbed aggregates is not significantly affected by the chloride counterion. Corresponding results are observed in the bulk solution, with spherical CTAB aggregates transformed to worm like structures at 80 mM KBr, while the corresponding change in aggregate structure is not observed for CTAC until an electrolyte concentration of 1200 mM KCl is reached [6].

The AFM investigation of Subramanian and Ducker [8] indicates that chloride ions have less influence on adsorbed surfactant structures than bromide ions. This study reported that the adsorbed aggregate structure did not deviate from spherical for LiCl concentrations up to at least 500 mM. The electrolyte co-ion differed in these experiments, however, results presented below will demonstrate that the electrolyte co-ion has little influence on adsorption behavior. Thus, it is reasonable to assume that the adsorbed layer structure is similar for 10 mM KCl and 10 mM LiCl. This assumption is in accordance with the CTAC and CTAC + KCl isotherms presented in Fig. 5.

Recall (cf. Fig. 2) that the  $c_{\text{sc}} > c_{\text{mc}}$  for CTAB and MTAB in the presence of 10 mM KBr. This was attributed to stabilization of semiformal interfacial structures by the electrolyte. This is not observed in Fig. 5 for the CTAC + KCl system. This result shows that it is not merely the presence of electrolyte in solution that affects this stabilization, but that the binding of the counterion to the adsorbed structure is all-important.

The kinetics of adsorption for CTAB, CTAB + KBr, CTAC and CTAC + KCl are presented in Fig. 6. It can be seen that the addition of electrolyte leads to an increase in the initial rate of adsorption for both the CTAC and CTAB system. This can be attributed to the screening of the electrostatic charge between the monomers and the surface. Note that very early in the adsorption process the surface charge is reversed as a result of surfactant adsorption. The raw adsorption rates for the surfactant systems exhibit a clear influence of the electrolyte type, while the surfactant plus electrolyte systems appear very similar. However, as discussed earlier it is more appropriate to compare the sticking ratio versus normalized concentration. This is shown in Fig. 7. In this figure it is readily apparent that electrolyte greatly increases the rate of adsorption. The CTAB + KBr result has been discussed earlier in connection with Fig. 4. Briefly cooperative

adsorption is seen up to the cmc, where a marked increase in sticking ratio indicates adsorption of micelles. Above the cmc competitive adsorption between micelles is observed. In the absence of KBr, similar trends are observed up to the cmc though the magnitude of the sticking ratio is reduced. Thus we conclude that for the CTAB and CTAB + KBr systems hydrophobic interactions are dominating the adsorption kinetics below the cmc and micelles adsorb directly to the surface above the cmc. In the absence of KBr, no competitive adsorption is seen between micelles. This is attributed firstly to the lower maximal surface excess in this system. Thus the surface is less crowded and competition for the surface is not observed and secondly to the greater proportion of monomers in the system that are competing with the micelles for adsorption.

The CTAC and CTAC + KCl systems exhibit very different behavior to CTAB. In both systems there is no increase in sticking ratio accompanying the cmc; thus there is no evidence of substantial levels of direct micellar adsorption. Recall that the ion binding of chloride is much reduced compared to bromide. Therefore the CTAC micelles carry a

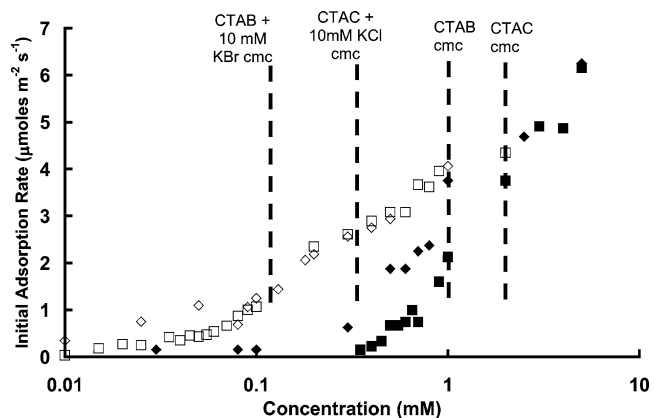


Fig. 6. Initial adsorption rate for CTAB in the presence (□) and absence (■) of 10 mM KBr and for CTAC in the presence (◇) and absence (◆) of 10 mM KCl.

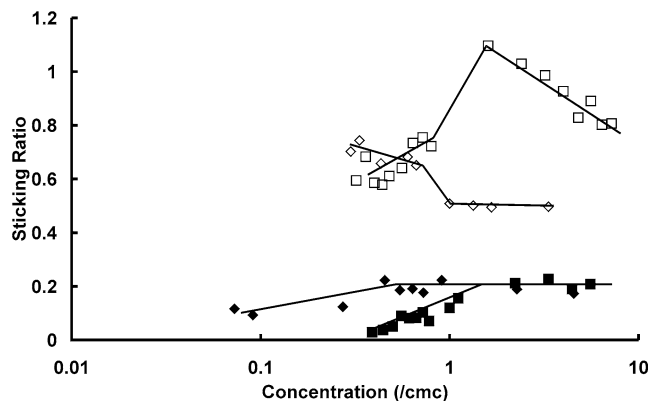


Fig. 7. Sticking ratio versus concentration normalized by the cmc for CTAB in the presence (□) and absence (■) of 10 mM KBr and for CTAC in the presence (◇) and absence (◆) of 10 mM KCl. The lines are drawn to guide the eye.

significantly larger surface charge than do CTAB micelles and the substrate will similarly have a greater charge. This will result in a greater electrostatic repulsion between the micelles and the substrate (once the surface charge of the latter has been reversed by adsorbed surfactant); therefore micellar adsorption will not be favored as it is in the CTAB system.

In the CTAC + KCl system below the cmc, the sticking ratio is seen to decrease with increasing concentration indicating competitive adsorption. In contrast, in the absence of KCl an increasing sticking ratio is seen below the cmc. The CTAC + KCl system has a higher cmc than the CTAB + KBr system. This results in a greater monomer concentration competing for adsorption and is indicative of predominantly electrostatic adsorption kinetics. Similar behavior was observed with MTAB and DTAB in KBr which also have a higher cmc than the CTAB + KBr system. Additionally the monomers must compete with the co-ion for electrostatic adsorption sites.

In the CTAC and CTAB systems the sticking ratio is much lower than in the electrolyte containing systems, reflecting the increased electrostatic repulsion between monomers and the surface. Additionally, the hydrophobic contribution to adsorption will be reduced in line with the increased cmc in the absence of electrolyte. However, cooperative adsorption is observed below the cmc indicating that hydrophobic interactions are more important than electrostatic interactions in the kinetics of adsorption for CTAC and CTAB in the absence of electrolyte.

### 3.3. The influence of the co-ion: $K^+$ , $Na^+$ , and $Li^+$

In this section the influence of the co-ion on adsorption behavior is investigated. The CTAC system has been chosen to investigate this effect, as it has been demonstrated in Fig. 5 and in the literature [4,8], that the addition of chloride ions has little influence on the maximal surface excess and the adsorbed aggregate morphology for CTAC.

Typical adsorption results for CTAC and CTAC in 10 mM NaCl, KCl and LiCl (henceforth referred to as CTAC and CTAC + NaCl, CTAC + KCl and CTAC + LiCl, or collectively as CTAC + XCl) are presented in Fig. 8. The surfactant concentration is  $0.45 \times \text{cmc}$  in each case, which corresponds to 0.5 mM for CTAC and 0.15 mM for CTAC + XCl. The form of the data is not significantly different to that described previously in Fig. 1, with equilibrium reached within a few seconds of surfactant being passed into the cell.

The adsorption isotherms for CTAC and the CTAC + XCl systems were also determined (not shown). The adsorption isotherms were shifted to lower concentrations in the presence of electrolyte, as noted previously for  $K^+$  in Fig. 5. Importantly, the size of this shift was independent of the co-ion type. The maximal surface excess up to 10 mM XCl was unaffected by the type of co-ion indicating that the co-ion has a minimal influence on the structure of the adsorbed aggregates. The rates of adsorption for CTAC and the CTAC + XCl systems were also determined. Once again, the results

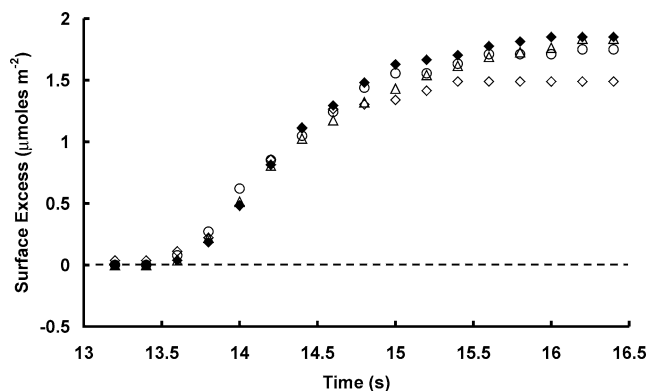


Fig. 8. Sample data for the adsorption of CTAC at the silica-solution interface versus time with 10 mM XBr. The surfactant concentrations are approximately  $0.45 \times \text{cmc}$  of each surfactant system. CTAC (0.5 mM) in the absence of electrolyte is represented by  $\blacklozenge$ , and 0.15 mM CTAC with 10 mM KCl, LiCl, and NaCl is represented by  $\diamond$ ,  $\circ$ , and  $\triangle$ , respectively. The surfactant solution is first passed into the cell at  $\sim 13.5$  s leading to adsorption. In all cases the equilibrium surface excess is reached within 3 s. The plateau level of adsorption is maintained while the surfactant solution is flowing into the cell.

for the three different co-ions were alike, indicating that the co-ion species has little effect on the adsorption rate.

These results are in agreement with the AFM study of Subramanian and Ducker [8] that demonstrated that the addition of LiCl up to a concentration of 500 mM had little effect on the adsorbed aggregate morphology of CTAC. Thus, it is expected that similar surface aggregate structures would be present for CTAC in the presence or absence of 10 mM XCl.

### 3.4. Slow secondary surfactant adsorption

Slow secondary increases in surface excess, similar to those described previously [9,10], have been elucidated for CTAC. The concentration range for slow adsorption or the SAR appears to be somewhat larger than for CTAB [9], with long-term increases in surface excess observed for 0.6–0.9 mM CTAC surfactant solutions. However, the most important result obtained in this investigation of CTAC adsorption is the first report of slow adsorption kinetics in the presence of electrolyte. This provides important clues as to the mechanism of slow adsorption.

The adsorption results presented in Fig. 9 for 0.6 and 0.7 mM CTAC are similar in form, with a fast initial increase in surface excess to approximately  $1.5 \mu\text{mol m}^{-2}$ , followed by a secondary increase to  $2.5 \mu\text{mol m}^{-2}$  over a period of 600 s. At this time equilibrium was attained and no further increases in surface excess were noted (see inset). The size of the secondary increase in adsorption for these concentrations is insufficient to bring about maximal levels of coverage, as was the case for 0.6 mM CTAB [9]. It is likely that an alternative in the adsorbed layer structure accounts for this difference. The change in surface excess that arises from secondary adsorption in the CTAC systems is less than that found previously in CTAB systems. However, the rate at

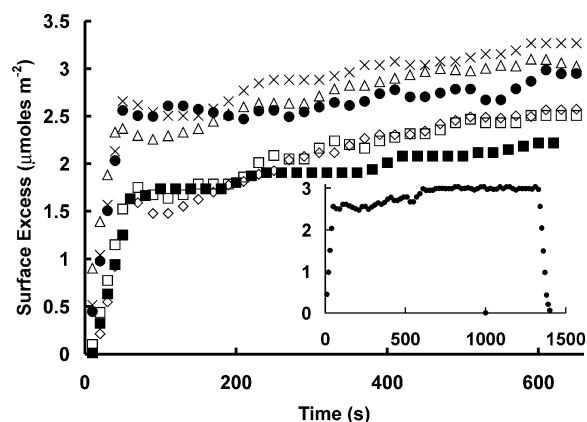


Fig. 9. Long-term adsorption results for CTAC. All CTAC solutions were monitored for a period of 3600 s, but as equilibrium adsorption levels were attained within 600 s, only this portion of the results is presented. The concentrations represented are 0.6 ( $\diamond$ ), 0.7 ( $\square$ ), 0.8 ( $\triangle$ ), and 0.9 mM ( $\times$ ). Importantly, a long-term result was noted in the presence of electrolyte for CTAC, for 0.25 mM CTAC in 10 mM LiCl ( $\bullet$ ). The first 600 s of the long-term result for 0.6 mM CTAB [9] ( $\blacksquare$ ) is also shown here for comparison. The inset shows the complete adsorption experiment for 0.25 mM CTAC in 10 mM LiCl and shows that there is no increase in surface excess after approximately 600 s.

which the secondary adsorption proceeds is similar, as can be seen in Fig. 9.

The rates of slow adsorption observed for 0.8 and 0.9 mM CTAC and 0.25 mM CTAC in the presence of LiCl are very similar. For these concentrations the fast initial increase is to a surface excess of  $2.5 \mu\text{mol m}^{-2}$ , so a more complete interfacial structure is present after the primary increase in adsorption than for the slightly lower concentrations. The magnitude of the secondary adsorption is decreased to approximately  $0.5 \mu\text{mol m}^{-2}$  for these concentrations, but this is sufficient to bring about maximal coverage of the substrate for the CTAC and CTAC + LiCl systems.

For both CTAC and CTAC + LiCl the long-term increases in adsorption occur in the vicinity of the  $c_{\text{SAC}}$  (as was the case for CTAB). The similarity in form of the data obtained for CTAB and CTAC supports the adsorption model postulated previously [9,10,14]. The fast initial increase in surface excess corresponds to neutralization and reversal of the exchangeable surface charge due to hydrophobic adsorption. The secondary increase in surface excess occurs as continued hydrophobic adsorption of monomers leads to the formation of complete (or perhaps semicomplete for CTAC) aggregates.

The observation of slow adsorption kinetics for CTAC in the presence of LiCl demonstrates that long-term increases in adsorption can occur in the presence of electrolyte, provided the electrolyte does not significantly alter the surface structure. Recall that the addition of 10 mM LiCl to CTAC solutions has no effect on the equilibrium surface excess and the adsorbed structure, nor does it permit increases in surface excess above the cmc. Thus, while the presence of 10 mM LiCl diminishes the electrostatic repulsion an adsorbing monomer experiences in the secondary adsorption

phase, the same structural barriers to adsorption are present as in the absence of electrolyte. This is evidence that it is the structural barrier to adsorption that is critical for the presence of a slow adsorption region in the isotherm.

Why then have long-term increases in adsorption not been elucidated for the other electrolyte co-ions? First,  $\text{K}^+$  and  $\text{Na}^+$  may have a small influence on the adsorbed surfactant morphology that is not revealed by a change in surface excess, and this change in morphology may permit more rapid adsorption to occur. Second, the addition of electrolyte not only lowers the solution cmc, but also narrows the concentration range of the increasing region of the isotherm; cf. Fig. 5. From a practical viewpoint this reduces the possibility of locating a concentration where long-term increases in adsorption occur. It is likely that with sufficiently precise investigations, an SAR could be found for NaCl, KCl and could be better defined for LiCl.

#### 4. Conclusions

Increasing the length of the surfactant hydrocarbon tail results in the adsorption isotherm being displaced to lower concentrations and an increase in the maximal surface excess. The addition of 10 mM KBr shifts the CTAB adsorption isotherm to lower concentrations and increases the maximal surface excess, therefore having a similar influence to an increase in chain length. The shift of the isotherm to lower concentrations is due to electrostatic screening of the headgroup charge which enables monomers to aggregate at lower surfactant concentrations. The increase in the maximal surface excess is associated with a change in structure of the adsorbed aggregates due to an increase in ion binding. For CTAC, while the addition of 10 mM KCl does shift the isotherm to lower concentrations, there is no corresponding elevation in the maximal surface excess. This is a consequence of the decreased binding efficiency of the chloride ion relative to the bromide ion. The bromide ion is able to drive a change in the surface aggregate structure, while the chloride ion is not. The co-ion species has been found to have little effect on the adsorption characteristics of CTAC, up to a bulk concentration of 10 mM XCl.

The rate of adsorption data shows that at any concentration longer chain length surfactants have a greater initial rate of adsorption. Thus hydrophobic interactions are seen to be increasingly important in the initial adsorption process as revealed by cooperative adsorption. The addition of electrolyte results in an increase in the adsorption rate due to a decrease in the electrostatic repulsion between the surfactant and the surface. The counterion also has important influences on the adsorption process as revealed by the adsorption kinetics. The high degree of ion binding of the bromide ion results in significant numbers of micelles adsorbing directly to the substrate. Additionally, the counterion type influences the adsorption kinetics below the cmc.

An SAR, previously reported for CTAB and CPBr, has also been detected for CTAC. Importantly, a slow adsorption result has been obtained for CTAC in the presence of 10 mM LiCl. This indicates that the origin of the slow adsorption kinetics is unlikely to be electrostatic in origin, and due to an energetic barrier associated with the need for a monomer to adopt a favorable orientation in the adsorbed aggregate structure.

## References

- [1] J.N. Israelachvili, D.J. Mitchell, *J. Chem. Soc. Faraday Trans.* 72 (1976) 1525.
- [2] T.P. Goloub, L.K. Koopal, *Langmuir* 13 (1997) 673.
- [3] L. Lajtar, J. Narkiewicz-Michalek, W. Rudzinski, *Langmuir* 9 (1993) 3174.
- [4] S.B. Velegol, B.D. Fleming, S. Biggs, E.J. Wanless, *Langmuir* 16 (2000) 2548.
- [5] D. Bartet, C. Gamboa, L. Sepulveda, *J. Phys. Chem.* 84 (1980) 272.
- [6] B. Lindman, M.C. Puyal, N. Kamenka, R. Rymden, *J. Phys. Chem.* 88 (1984) 5048.
- [7] L.J. Magid, Z. Han, G.G. Warr, M.A. Cassidy, P.D. Butler, W.A. Hamilton, *J. Phys. Chem. B* 101 (1997) 7919.
- [8] V. Subramanian, W.A. Ducker, *Langmuir* 16 (2000) 4447.
- [9] R. Atkin, V.S.J. Craig, S. Biggs, *Langmuir* 16 (2000) 9374.
- [10] R. Atkin, V.S.J. Craig, S. Biggs, *Langmuir* 17 (2001) 6155.
- [11] M. Chorro, C. Chorro, O. Dolladille, S. Partyka, R. Zana, *J. Colloid Interface Sci.* 199 (1998) 169.
- [12] J. Penfold, E. Staples, I. Tucker, *Langmuir* 18 (2002) 2967.
- [13] T.P. Goloub, L.K. Koopal, B.H. Bijsterbosch, M.P. Sidorova, *Langmuir* 12 (1996) 3188.
- [14] R. Atkin, V.S.J. Craig, E.J. Wanless, S. Biggs, *Adv. Colloid Interface Sci.* 103 (2003) 219.
- [15] R.K. Iler, *The Chemistry of Silica*, Wiley–Interscience, New York, 1979.
- [16] J.C. Dijt, M.A. Cohen Stuart, J.E. Hofman, G.J. Fleer, *Colloids Surf.* 51 (1990) 141.
- [17] T. Dabros, T.G.M. van de Ven, *Colloid Polym. Sci.* 261 (1983) 694.
- [18] D.R. Lide, *Handbook of Chemistry and Physics*, CRC Press, Boca Raton, FL, 1995.
- [19] E.S. Pagac, D.C. Prieve, R.D. Tilton, *Langmuir* 14 (1998) 2333.
- [20] J. Briggs, R.B. Dorshow, *J. Chem. Phys.* 76 (1982) 775.
- [21] P. Somasundaran, D.W. Fuerstenau, *J. Phys. Chem.* 70 (1966) 90.
- [22] R. Atkin, V.S.J. Craig, E.J. Wanless, S. Biggs, *J. Phys. Chem. B* 107 (2003) 2978.